



Characterization and photocatalytic activity of poly(3-hexylthiophene)-modified TiO₂ for degradation of methyl orange under visible light

Desong Wang^{a,*}, Jie Zhang^a, Qingzhi Luo^b, Xueyan Li^b, Yandong Duan^a, Jing An^b

^a College of Chemical and Pharmaceutical Engineering, Hebei University of Science and Technology, Shijiazhuang, Hebei 050018, PR China

^b College of Science, Hebei University of Science and Technology, Shijiazhuang, Hebei 050018, PR China

ARTICLE INFO

Article history:

Received 12 September 2008

Received in revised form

25 December 2008

Accepted 30 March 2009

Available online 5 April 2009

Keywords:

Photocatalytic activity

Titanium dioxide

Methyl orange degradation

Poly(3-hexylthiophene)

ABSTRACT

Poly(3-hexylthiophene) (P3HT) was synthesized via chemical oxidative polymerization with anhydrous FeCl₃ as oxidant, 3-hexylthiophene as monomer, chloroform as solvent. TiO₂ nanoparticles modified by a small amount of P3HT (TiO₂/P3HT) were prepared by blending TiO₂ nanoparticles and P3HT in chloroform solution. The resulting photocatalysts were characterized by the methods of TEM, XRD, FT-IR, XPS and UV–vis diffuse reflectance spectroscopy. The photocatalytic activity of TiO₂/P3HT was investigated by degrading methyl orange under visible light. The degradation rate of methyl orange was 88.5 and 13.5% when it was degraded by TiO₂/P3HT and neat TiO₂(P-25) for 10 h, respectively. In addition, TiO₂/P3HT nanocomposites showed excellent photocatalytic stability after 10 cycles under visible light irradiation. A possible mechanism for the photocatalytic oxidative degradation was also discussed.

© 2009 Elsevier B.V. All rights reserved.

1. Introduction

In the field of environmental chemistry, semiconductor mediated photocatalysis has been the focus of recent attention since it aims at the destruction of contaminants in water and air [1]. Among the semiconductors, titanium dioxide (TiO₂) is an excellent photocatalyst, because it is an effective, photostable, reusable, inexpensive, non-toxic and easily available catalyst [2]. However, the wide band gap (3.2 eV) of TiO₂ only allows it to absorb the ultraviolet light (<387 nm) that limits the utilization of solar light since UV light in solar light is less than 5%. Hence, much effort has been devoted to developing a TiO₂-based photocatalyst which is capable of efficient utilization of the visible light.

To extend the photoresponse of TiO₂ to the visible region, many modification methods, such as metal ion doping [3], non-metal doping [4], noble metal deposition [5–7], composite semiconductors [8–10], surface dye sensitization [11] and photosensitive material modification [12] have been reported. Recently, a little work has been done on using conjugated polymer-modified TiO₂ to degrade organic pollutant since nanocomposites of conductive polymers and inorganic particles show interesting physical properties and application potential [13–16]. Some studies have been published on the combination of conductive polymer and TiO₂ to improve their performance of UV light and sunlight activities [17–20].

For example, Li et al. reported that a series of polyaniline–TiO₂ nanocomposite powders with different PANI/TiO₂ ratios were prepared and their photocatalytic degradation of phenol under visible light irradiation was investigated [21]. Wang et al. found that TiO₂/polypyrrole nanocomposite particles possessed good sunlight photocatalytic activities [22]. Muktha et al. investigated the preparation of a nanocomposite film with poly(3-hexylthiophene) (P3HT) as matrix and TiO₂ nanoparticles as doping agent, and found that the nanocomposite film had good photocatalytic activities when degrading a common dye under UV exposure [23]. To the best of our knowledge, little work has been done on the photocatalytic activity of TiO₂ nanoparticles modified by P3HT under visible light irradiation. In this paper, we have prepared TiO₂ nanoparticles modified by a small amount of P3HT (TiO₂/P3HT) and investigated the visible light photocatalytic activities of TiO₂/P3HT.

2. Experimental

2.1. Materials

TiO₂ (P-25, Degussa Corporation, Germany) having a specific surface area of 50 m²/g was dried at 100 °C for 4 h prior to use. 3-Hexylthiophene was commercially purchased from Synwit Technology Co., Ltd., China (purity >98%), and was distilled under reduced pressure prior to use. Anhydrous FeCl₃ (Shanghai, Chemical Reagent Co., Ltd., China), chloroform and all other chemicals (Tianjin Chemical Reagent Co., Ltd., China) were of analytical reagent grade and used without further purification.

* Corresponding author. Tel.: +86 311 81669901; fax: +86 311 88632016.

E-mail address: dswang06@126.com (D. Wang).

2.2. Synthesis of TiO₂/P3HT nanocomposites

The TiO₂/P3HT nanocomposites were prepared according to the following steps: first, poly(3-hexylthiophene) (P3HT) was synthesized via chemical oxidative polymerization with anhydrous FeCl₃ as oxidant, 3-hexylthiophene as monomer, chloroform as solvent by the reported procedure [24]. Then, 2.0 g TiO₂ nanoparticles (Degussa P-25) were added to chloroform solutions (50 mL) of P3HT with the different molar ratios of Degussa P-25 titania to 3-hexylthiophene (30:1, 50:1, 75:1, 100:1, 125:1). After continuously ultrasonicated for 3 h, the above suspension mixtures were filtered. Finally, the product was dried at 60 °C under vacuum till the constant mass was reached.

2.3. Characterizations

Transmission electron microscopy (TEM) study was carried out on a Tecnai G2 F20 electron microscopy instrument. The samples of TEM were prepared by dispersing the final nanoparticles in ethanol; the suspension was then dropped on carbon–copper grids.

X-ray diffraction (XRD) patterns of TiO₂/P3HT nanocomposites were measured in the range of $2\theta = 5\text{--}80^\circ$ by step scanning on the Rigaku D/MAX-2500 diffractometer (Rigaku Co., Japan) with Cu K α radiation ($k = 0.15406$ nm) operated at 40 kV and 100 mA.

Fourier transform infrared spectra (FT-IR) of the samples were recorded on spectrometer (SHIMADZU) in the range of 4000–400 cm⁻¹. Measurements were performed in the transmission mode in spectroscopic grade KBr pellets for all the powders.

X-ray photoelectron spectrometer (XPS) was performed on a PerkinElmer PHI 1600 ESCA system with an Mg K α X-ray source.

A Varian Cary 100 Scan UV–vis system equipped with an integrating sphere attachment was used to obtain the reflectance spectra of the catalysts over a range of 200–800 nm. Integrating sphere USRS-99-010 was employed as a reflectance standard.

2.4. Photocatalytic activity

The photodegradation of methyl orange (MO) was used to evaluate the visible light photocatalytic activities of TiO₂/P3HT catalysts. Aqueous methyl orange solution (450 mL) with an initial concentration of 10 mg/L was put into a cylindrical glass vessel. Then TiO₂/P3HT nanocomposites (0.45 g) were added into the glass vessel with a circulating water jacket to maintain constant temperature. Before irradiation, the suspensions containing MO and catalysts were continuously stirred for 2 h at dark in order to reach an adsorption–desorption equilibrium. After that, the system was subjected to visible light which was obtained by a 300 W iodine tungsten lamp (Philips, China) with a 400 nm cutoff filter to ensure the desired irradiation light. The glass reactor was open to air to ensure enough oxygen into the reaction solution. The distance between the surface of the solution and the light source was about 10 cm. During irradiation, each sample was taken out every 2 h. TiO₂/P3HT nanocomposite particles were separated from the mixture solution with centrifugation at 10,000 rpm for 10 min. The clarified solution was analyzed by 723 UV–vis spectrometer (Shanghai Spectrum Instruments Co., Ltd., China) to obtain the absorbance of MO at a wave length of 464 nm, corresponding to maximum absorption wavelength of MO. The concentration of MO was calculated by a calibration curve. The reactions were carried out at natural pH conditions. The degradation rate (%) could be calculated as the following equation:

$$D = \frac{c_0 - c_t}{c_0} \times 100\% \quad (1)$$

where D is degradation rate, c_0 and c_t are the concentration of methyl orange solution before and after irradiation, respectively.

3. Results and discussion

3.1. TEM images

The TEM images of neat TiO₂ and P3HT-modified TiO₂ nanoparticles are clearly displayed in Fig. 1(a) and (b). It can be confirmed that the morphology of the composites is similar to that of neat TiO₂. In addition, the modification of P3HT does not change the size of neat TiO₂ significantly. The mean sizes of both nanoparticles are 20–30 nm approximately.

3.2. XRD patterns

The XRD patterns of TiO₂ and TiO₂/P3HT are shown in Fig. 2. It can be seen that there are little difference between curves (a) and (b) in shape and position of the diffraction peaks. The amount of P3HT is so small that no diffraction peaks of P3HT are observed in curve (b). Results imply that the crystalline phase of

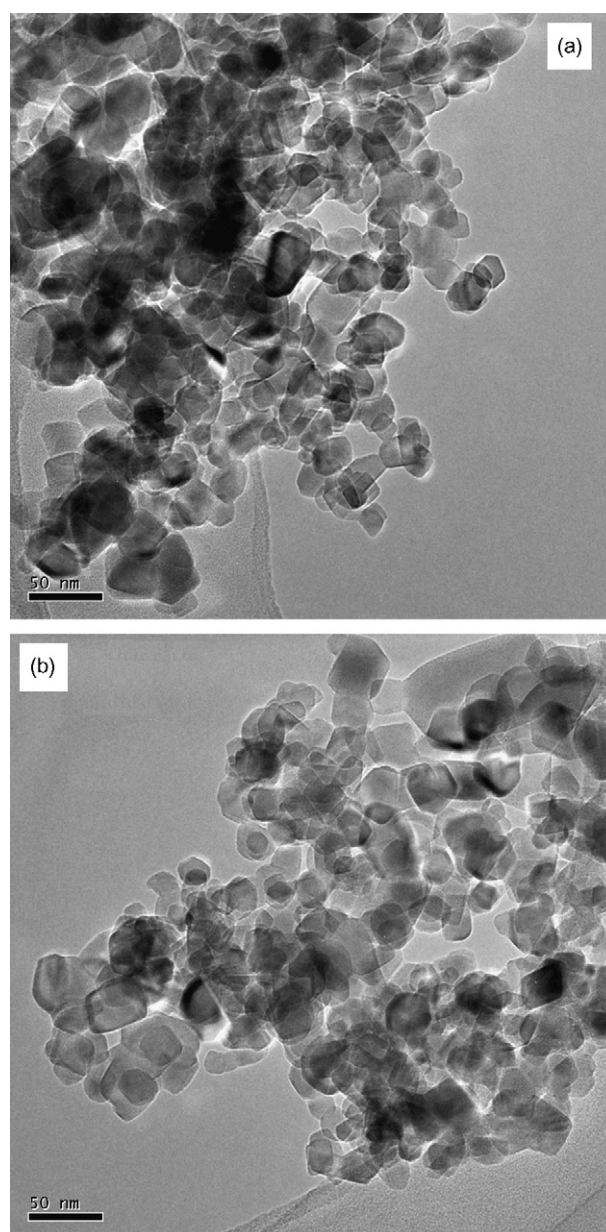


Fig. 1. TEM images of neat TiO₂ (a) and TiO₂/P3HT (b) (75:1).

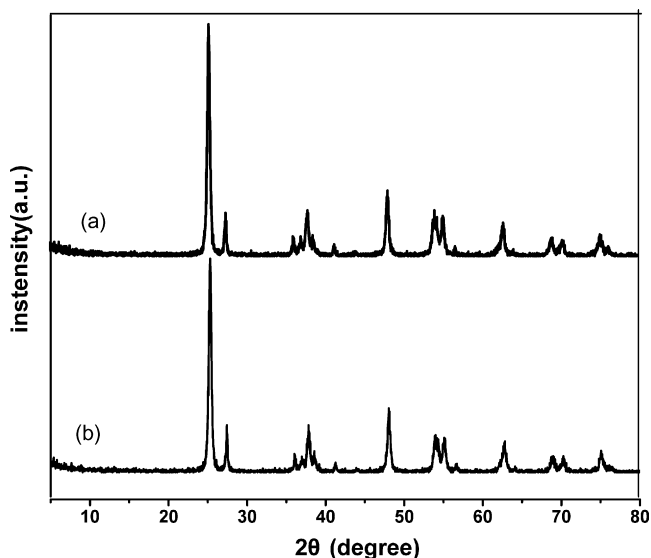


Fig. 2. X-ray diffraction patterns of TiO_2 nanoparticles (a) and $\text{TiO}_2/\text{P3HT}$ nanocomposite (b) (75:1).

TiO_2 has not been changed by the modification of $\text{TiO}_2/\text{P3HT}$. The mean sizes of TiO_2 nanoparticles and $\text{TiO}_2/\text{P3HT}$ nanocomposites, calculated by Scherrer's formula, are 20 and 22 nm, respectively, which are approximately consistent with the results of TEM analyses.

3.3. FT-IR analysis

The FT-IR absorption spectra of P3HT, TiO_2 and $\text{TiO}_2/\text{P3HT}$ are shown in Fig. 3. The main characteristic peaks of P3HT appear in the spectrum of $\text{TiO}_2/\text{P3HT}$ nanocomposite as follows: The band at 2926 cm^{-1} is associated with the C–H stretching mode of the thiophene rings; 2856 cm^{-1} is based on hexyl C–H stretching absorption; while the absorption peaks at 1459 and 1419 cm^{-1} are attributed to the C=C stretching vibration on the thiophene ring. The wide peak at $420\text{--}800\text{ cm}^{-1}$ corresponds to Ti–O bending mode of TiO_2 . The characteristic peaks of P3HT and TiO_2 can be found in the spectrum of $\text{TiO}_2/\text{P3HT}$ nanocomposite.

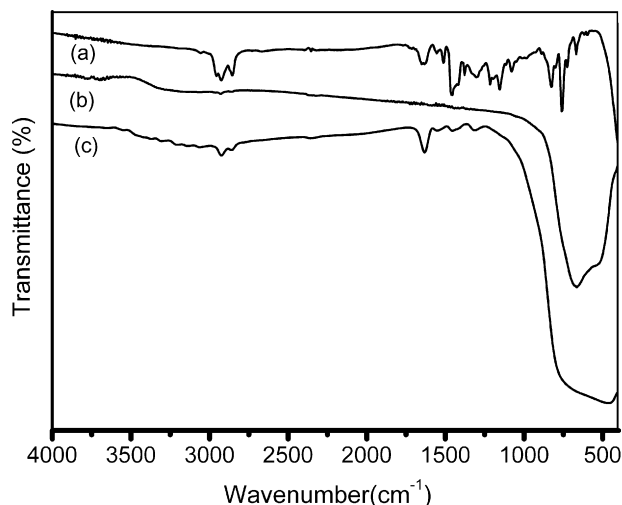


Fig. 3. FT-IR spectra of P3HT (a), TiO_2 (b) and $\text{TiO}_2/\text{P3HT}$ composite (c) (75:1).

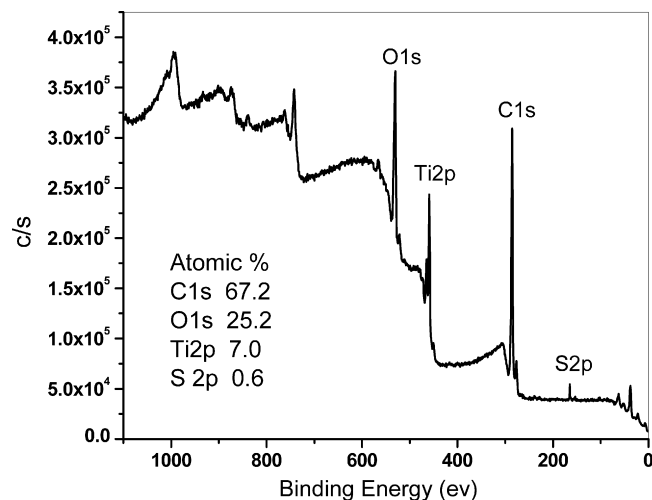


Fig. 4. XPS spectrum of $\text{TiO}_2/\text{P3HT}$ (75:1).

3.4. X-ray photoelectron spectroscopy

XPS analysis is used to determine the chemical states and content of each element possibly existing in the samples. Fig. 4 shows the XPS survey spectra of $\text{TiO}_2/\text{P3HT}$ (75:1). Elements of C, O, Ti and S are confirmed to exist in the nanocomposites by the four peaks at binding energies of 284.8, 529.8, 458.6 and 164.0 eV, which are related to C1s, O1s, Ti2p and S2p, respectively. The mass contents of C, O, Ti and S are 67.2, 25.2, 7.0, 0.6%, respectively, suggesting that P3HT exists in the surface of nanocomposite particles.

3.5. UV-vis diffuse reflectance spectra

Fig. 5 shows the UV-vis DRS spectra of the samples. It could be observed that P3HT-modified TiO_2 could lead to response to visible light. In addition, the onsets of absorption edge are calculated by the intercept of the drawn tangent on the wavelength axis, which are at 388, 414, 410, 407 and 396 nm for the samples of neat TiO_2 , $\text{TiO}_2/\text{P3HT}$ (30:1), $\text{TiO}_2/\text{P3HT}$ (50:1), $\text{TiO}_2/\text{P3HT}$ (75:1), $\text{TiO}_2/\text{P3HT}$ (100:1), respectively. Accordingly, the corresponding band gap energies are 3.2, 2.99, 3.02, 3.04 and 3.13 eV. Results show the band gap energies of all the $\text{TiO}_2/\text{P3HT}$ nanocomposites are lower than that of neat TiO_2 , so the $\text{TiO}_2/\text{P3HT}$ nanocomposites can be excited to produce more electron-hole pairs under visible

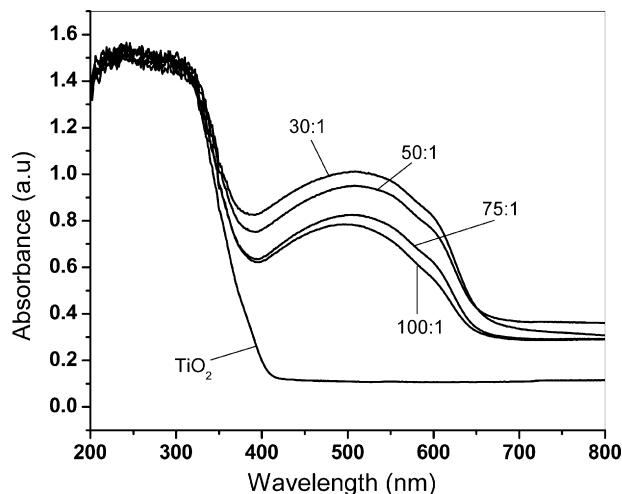


Fig. 5. UV-vis diffuse reflectance spectra of neat TiO_2 and $\text{TiO}_2/\text{P3HT}$ (75:1).

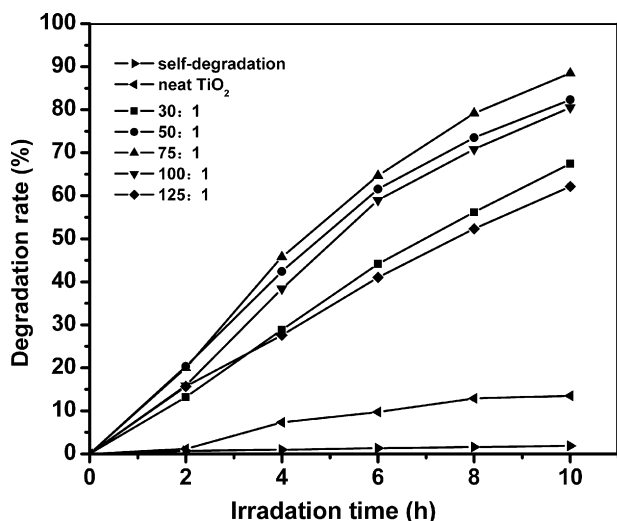


Fig. 6. Comparison of the photocatalytic degradation of MO in presence of TiO₂/P3HT (30:1), (50:1), (75:1), (100:1), (125:1), TiO₂ and self-degradation of MO under visible light irradiation.

light, which could result in higher visible light photocatalytic activities. Therefore, UV–vis DRS spectra indicate that the TiO₂/P3HT nanocomposite is a promising material for the full use of visible light.

3.6. Photocatalytic activity

Fig. 6 shows the photocatalytic activities of neat TiO₂ and TiO₂/P3HT nanocomposites with different molar ratios of TiO₂ to P3HT under visible light irradiation. It is found that the self-degradation of methyl orange is negligible, the degradation rate for neat TiO₂ sample is only 13.5% in 10 h, while TiO₂/P3HT exhibits much higher degradation rate than neat TiO₂, indicating that TiO₂/P3HT possesses better photocatalytic activity under visible light. The degradation rate of methyl orange increases at first and then decreases with the increasing of the molar ratio of TiO₂/P3HT from 30:1 to 125:1, and reaches the maximum of 88.5% in 10 h when the molar ratio of TiO₂/P3HT is 75:1. The improvement of visible light photocatalytic performance of TiO₂/P3HT is similar to that of PANI/TiO₂ photocatalyst [25].

3.7. Photocatalytic stability of TiO₂/P3HT

The photocatalytic stability of TiO₂/P3HT nanocomposites was performed with the concentration of MO (10 mg/L), catalyst dosage (1 g/L) and irradiation time (10 h) for each cycling run. The regeneration of the photocatalyst was done by filtrating the suspension to remove the bulk solution, and drying at 60 °C for 10 h. The recovered TiO₂/P3HT nanocomposites were reused in the next cycle. The results displayed in Fig. 7 show that after 10 successive cycles under the visible light irradiation, the degradation rate of MO is still 60% of that of the first cycling run, indicating that TiO₂/P3HT nanocomposites possess excellent photocatalytic stability.

3.8. Photocatalytic mechanism

The relative energy level of P3HT (π -orbital and π^* -orbital) and TiO₂ (conduction band, CB, and valence band, VB) is shown in Scheme 1. Based on the results of photocatalytic tests, the photocatalytic mechanism under visible light irradiation can be inferred as follows. P3HT absorbs visible light to induce electron π - π^* transition. The excited-state electrons are transported from π -orbital to π^* -orbital. The d-orbital (CB) of TiO₂ and π^* -orbital of P3HT match

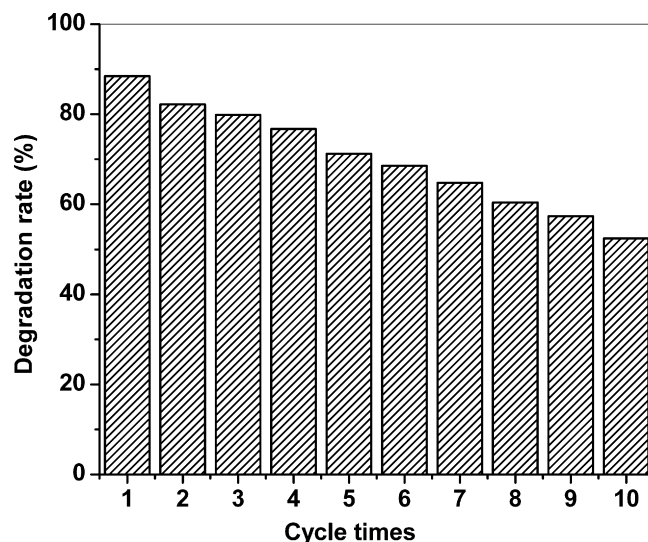
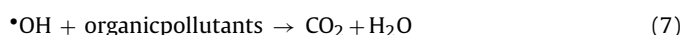
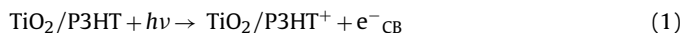
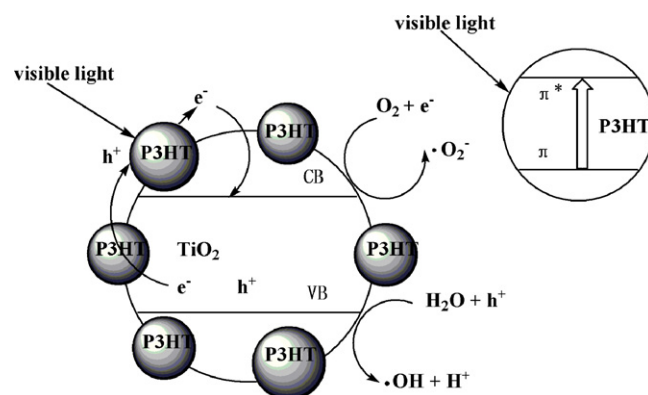


Fig. 7. Photocatalytic degradation rate of methyl orange with TiO₂/P3HT (75:1) composite in different recycling time.

well in energy level, which can cause synergic effect. Based on the synergic effect, the excited-state electrons could be injected into the d-orbital (CB) of TiO₂ readily and transferred to the nanocomposite surface to react with oxygen to yield superoxide radicals $\cdot\text{O}_2^-$ subsequently. At the same time, a positive charged hole (h^+) might be formed by electron migrating from TiO₂ valence band to P3HT π -orbital, which can react with OH⁻ or H₂O to generate $\cdot\text{OH}$. It is the super-oxide radical ion $\cdot\text{O}_2^-$ and hydroxyl radical $\cdot\text{OH}$ that are responsible for the degradation of organic compounds [25]. The whole process can be clearly described in Scheme 1. The reactions can be expressed as follows:



The band gap of P3HT is 1.9 eV and the corresponding wavelength is 653 nm [26], which indicates that P3HT shows strong absorption in visible light region. Based on the above UV–vis diffuse reflectance



Scheme 1. Mechanism of TiO₂/P3HT composites to enhance the photocatalytic activity under visible light.

spectra, it can be seen that the band gap of the nanocomposites are narrower than that of neat TiO₂ (3.2 eV). Hence, P3HT may be as a photosensitizer for TiO₂ [27].

4. Conclusions

P3HT was synthesized via chemical oxidative polymerization. TiO₂/P3HT nanocomposites were successfully prepared by blending TiO₂ and P3HT in chloroform solution. The size and shape of neat TiO₂ and TiO₂/P3HT nanocomposites are displayed by TEM images and XRD patterns. The results of XRD indicate that the modification does not change the crystalline phase of neat TiO₂. XPS and FT-IR analysis suggest that P3HT exists on the surface of nanocomposites. UV–vis diffuse reflectance spectra confirm that the modified catalysts possess a strong absorption band in the visible range of 400–700 nm. Results of degradation show that the photocatalytic activity of the nanocomposites is much higher than that of neat TiO₂. Photocatalytic stability tests indicate that TiO₂/P3HT nanocomposites possess excellent photocatalytic stability. Photocatalytic mechanism reveals P3HT might be a photosensitizer for TiO₂ to decrease the band gap energy of TiO₂ and improve the photocatalytic activity.

Appendix A. Supplementary data

Supplementary data associated with this article can be found, in the online version, at doi:10.1016/j.jhazmat.2009.03.135

References

- [1] T. Oppenlaender, Photochemical Purification of Water and Air, Wiley-VCH Verlag, Weinheim, Germany, 2003.
- [2] H.M. Yang, K. Zhang, R.R. Shi, X.W. Li, X.D. Dong, Y.M. Yu, Sol–gel synthesis of TiO₂ nanoparticles and photocatalytic degradation of methyl orange in aqueous TiO₂ suspensions, *J. Alloys Compd.* 413 (2006) 302–306.
- [3] T.Z. Tong, J.L. Zhang, B.Z. Tian, F. Chen, D.N. He, Preparation of Fe³⁺-doped TiO₂ catalysts by controlled hydrolysis of titanium alkoxide and study on their photocatalytic activity for methyl orange degradation, *J. Hazard. Mater.* 155 (2008) 572–579.
- [4] J.H. Sun, L.P. Qiao, S.P. Sun, G.L. Wang, Photocatalytic degradation of Orange G on nitrogen-doped TiO₂ catalysts under visible light and sunlight irradiation, *J. Hazard. Mater.* 155 (2008) 312–319.
- [5] Y. Ishibai, J. Sato, T. Nishikawa, S. Miyagishi, Synthesis of visible-light active TiO₂ photocatalyst with Pt-modification: role of TiO₂ substrate for high photocatalytic activity, *Appl. Catal. B* 79 (2008) 117–121.
- [6] L. Ge, M.X. Xu, Influences of the Pd doping on the visible light photocatalytic activities of InVO₄-TiO₂ thin films, *Mater. Sci. Eng. B* 131 (2006) 22–229.
- [7] Z.L. Jin, X.J. Zhang, G.X. Lu, S.B. Li, Improved quantum yield for photocatalytic hydrogen generation under visible light irradiation over eosin sensitized TiO₂—investigation of different noble metal loading, *J. Mol. Catal. A: Chem.* 259 (2006) 275–280.
- [8] Y.J. Zhang, W. Yan, Y. Wu, P. Zhen, H. Wang, Synthesis of TiO₂ nanotubes coupled with CdS nanoparticles and production of hydrogen by photocatalytic water decomposition, *Mater. Lett.* 23 (2008) 3846–3848.
- [9] H. Shinguu, M.M.H. Bhuiyan, T. Ikegami, K. Ebihara, Preparation of TiO₂/WO₃ multilayer thin film by PLD method and its catalytic response to visible light, *Thin Solid Films* 506–507 (2006) 111–114.
- [10] Y.H. Xu, Z.X. Zeng, The preparation, characterization, and photocatalytic activities of Ce–TiO₂/SiO₂, *J. Mol. Catal. A: Chem.* 279 (2008) 77–81.
- [11] K.S. Yao, D.Y. Wang, C.Y. Chang, K.W. Weng, L.Y. Yang, S.J. Lee, T.C. Cheng, C.C. Hwang, Photocatalytic disinfection of phytopathogenic bacteria by dye-sensitized TiO₂ thin film activated by visible light, *Surf. Coat. Technol.* 202 (2007) 1329–1332.
- [12] Y.J. Zang, R. Farnood, Photocatalytic activity of AgBr/TiO₂ in water under simulated sunlight irradiation, *Appl. Catal. B* 79 (2008) 334–340.
- [13] Q.T. Vu, M. Pavlik, N. Hebestreit, U. Rammelt, W. Plieth, J. Pfleger, Nanocomposites based on titanium dioxide and polythiophene: structure and properties, *React. Funct. Polym.* 65 (2005) 69–77.
- [14] M.U. Jurczyk, A. Kumar, S. Srinivasan, E. Stefanakos, Polyaniline-based nanocomposite materials for hydrogen storage, *Int. J. Hydrogen Energy* 32 (2007) 1010–1015.
- [15] J.S. Salafsky, W.H. Lubberhuizen, R.E.I. Schropp, Photoinduced charge separation and recombination in a conjugated polymer-semiconductor nanocrystal composite, *Chem. Phys. Lett.* 290 (1998) 297–303.
- [16] A.C. Arango, S.A. Carter, P. Brock, Charge transfer in photovoltaics consisting of interpenetrating networks of conjugated polymer and TiO₂ nanoparticles, *J. Appl. Phys. Lett.* 74 (1999) 1698.
- [17] S.X. Xiong, Q. Wang, H.S. Xia, Template synthesis of polyaniline/TiO₂ bilayer microtubes, *Synth. Met.* 146 (2004) 37–42.
- [18] L.X. Zhang, P. Liu, Z.X. Su, Preparation of PANI–TiO₂ nanocomposites and their solid-phase photocatalytic degradation, *Polym. Degrad. Stab.* 91 (2006) 2213–2219.
- [19] J. Li, L.H. Zhu, Y.H. Wu, Y. Harima, A.Q. Zhang, H.Q. Tang, Hybrid composites of conductive polyaniline and nanocrystalline titanium oxide prepared via self-assembling and graft polymerization, *Polymer* 47 (2006) 7361–7367.
- [20] F. Wang, S.X. Min, TiO₂/polyaniline composites: an efficient photocatalyst for the degradation of methylene blue under natural light, *Chin. Chem. Lett.* 18 (2007) 1273–1277.
- [21] X.Y. Li, D.S. Wang, G.X. Cheng, Q.Z. Luo, J. An, Y.H. Wang, Preparation of polyaniline-modified TiO₂ nanoparticles and their photocatalytic activity under visible light, *Appl. Catal. B* 81 (2008) 267–273.
- [22] D.S. Wang, Y.H. Wang, X.Y. Li, Q.Z. Luo, J. An, J.X. Yue, Sunlight photocatalytic activity of polypyrrole–TiO₂ nanocomposites prepared by ‘in situ’ method, *Catal. Commun.* 9 (2008) 1162–1166.
- [23] B. Muktha, D. Mahanta, S. Patil, G. Madras, Synthesis and photocatalytic activity of poly(3-hexylthiophene)/TiO₂ composites, *J. Solid State Chem.* 180 (2007) 2986–2989.
- [24] R.D. McCullough, R.D. Lowe, M. Jayaraman, D.L. Anderson, Design, synthesis, and control of conducting polymer architectures: structurally homogeneous poly(3-alkylthiophenes), *J. Org. Chem.* 58 (1993) 904.
- [25] H. Zhang, R.L. Zong, J.A. Zhao, Y.F. Zhu, Dramatic visible photocatalytic degradation performances due to synergetic effect of TiO₂ with PANI, *Environ. Sci. Technol.* 42 (10) (2008) 3803–3807.
- [26] L.J.A. Koster, V.D. Mihailetschi, P.W.M. Blom, Ultimate efficiency of polymer/fullerene bulk heterojunction solar cells, *Appl. Phys. Lett.* 88 (2006) 093511.
- [27] S. Lin, R.L. Qiu, Y.Q. Mo, D.D. Zhang, H. Wei, Y. Xiong, Photodegradation of phenol in a polymer-modified TiO₂ semiconductor particulate system under the irradiation of visible light, *Catal. Commun.* 8 (2007) 429–433.